Does the Interfacial Potential Control the Charge Separation Efficiency in Reverse Micellar Media?

D. Grand* and A. Dokutchaev†

URA 75, CNRS Université de Paris Sud, 91 405 Orsay Cedex, France

Received: November 21, 1996; In Final Form: February 18, 1997[⊗]

The effect of the water pool size ($\omega°$) on the average number of the probe molecules located at the interface and on the monophotonic ionization yield has been examined in anionic and cationic reverse micelles, using tetramethylbenzidine (TMB) as an easily photoionizable solute. The main conclusions of the present study are as follows: (1) The number of molecules located at the interface parallels that of the square radius of the water pool and partly depends on the compactness of the interface. (2) Owing to the high concentration of the counterions, the variations of the electrical potential remain low, when $\omega°$ increases from 18 to 40, although the fraction of free water increases significantly. (3) The charge separation efficiency (Y_{TMB^+}) varies as the fraction of free water in the water pool. Such Y_{TMB^+} variations are interpreted in changes in the fundamental energy of the excess electron at the interface with $\omega°$. (4) The comparison of Y_{TMB^+} values, obtained in the present work with previous data in direct micelles, points out the influence of the sign of the curvature radius on the photoionization reaction.

Introduction

Ionization is one of the simplest chemical reactions. Photoionization of different solutes, induced by absorption of photons of low energy, has been extensively studied in various homogeneous solutions. As a result, the energy threshold (E_{th}), the quantum yield (φ_{ion}) of the charge separation process, as well as the shape of the ionization efficiency curves pointed out the influence of the environment. These studies showed also that the E_{th} value is largely determined by a variation of V_0, the fundamental energy of the electron formed in a quasi-free state.[1−4] Thus, photoionization of embedded chromophores appeared as an attractive tool in the comprehension of the interfacial effects when the charge separation occurs at an interface.

In binary systems, such as direct micelles (Mi) or vesicles (Ve), at room temperature it was shown that the φ_{ion} values depend on the electrical potential variations ($\Delta\psi$) in the case of anionic micelles or vesicles,[5,6] whereas in cationic Mi^+, the major photophysical process was the triplet formation of the excited probe,[7] and the electron ejection into water appeared to be facilitated by the water organization at the interface.[8]

In ternary systems, such as swollen direct micelles and reverse micelles, it was also displayed that the ejection of an electron from a micellized chromophore occurs into the aqueous phase.[6,9−11] The solvation time,[12] the spectroscopic properties, the yield, and the decay of the hydrated electron[9,11,13] were found to be dependent on the $\omega°$ value with $\omega° = [H_2O]/[\text{surfactant}]$.

It was also observed that the sequestered water presents a microstructure which depends on the water pool size $\omega°$ of the reverse micelle.[14−17]

In fact, in reverse micelles and at room temperature, little is known about the influence of $\omega°$ on the variations of the interfacial potential ($\Delta\psi$) as well as on the number of chromophore molecules located at the interface and hence on their charge separation efficiency.

It is the purpose of the present work, through the study of the photoionization of tetramethylbenzidine (TMB) in anionic and cationic reverse micelles.

Experimental Section

1. Materials. The surfactants (Sur) were used as purchased from Fluka: sodiumdiethylsulfosuccinate (AOT, purity > 99%) and benzyldimethylhexadecylammonium chloride (BHDC, purity > 97%). The surfactant concentration was kept constant: 0.15 M for AOT and 0.27 M for BHDC.

The solvents (*n*-heptane, benzene) were of the highest purity available (Fluka, UV spectrograde quality) and were used without further purification.

The probes (Pr) were used as received: *N*,*N*,*N*′,*N*′-tetramethylbenzidine (TMB, Sigma) and pyrene-1-carboxaldehyde (PyCHO, Aldrich). TMB displays numerous attractive properties: a low gas-phase ionization potential,[18] a high φ_{ion} in solutions when the photon energy is higher than the energy threshold of photoionization, a cation TMB^+ with a large extinction coefficient at 474 nm ($\epsilon = 40\,000\ M^{-1}\ cm^{-1}$), and a long lifetime in polar organic solvents.[7,19] The dry TMB was incorporated into the hydrocarbon solvent, and the solution was then filtered. The TMB concentration was $\sim 10^{-3}$ M, on the basis of an $\epsilon_{(\lambda max)} = 34\,000\ M^{-1}\ cm^{-1}$ in benzene or *n*-heptane.

Dilute solutions of PyCHO ($<10^{-4}$ M) were used in fluorescence experiments.

2. Sample Preparation. The reverse micelle was prepared by dissolving and mixing for ca. 30 min a known volume of dissolved water (resistivity = 18.2 MΩ cm) in Sur/Pr/hydrocarbon solutions. All experiments were performed with freshly prepared solutions, and each point was the result of about 6 runs. If necessary, oxygen was removed by flushing the micellar solution with 99.9% argon for 30 min prior to laser excitation. Table 1 gathers the characteristics of both micelles versus $\omega°$ variations, as taken from refs 20−23, 40.

3. Apparatus. Nanosecond photolysis was carried out with a neodynium YAG laser, tripled to 353 nm (flash duration of 7 ns). The pulse energy was fixed at about 45 mJ to avoid biphotonic ionization of the TMB_{bulk} solubilized in the hydro-

† On leave from Mendeleev Institute of Chemical Technology, Moscow, CEI.

[⊗] Abstract published in *Advance ACS Abstracts,* April 1, 1997.

S1089-5647(96)03884-9 CCC: $14.00

TABLE 1: Size Parameters of the Reverse Micelles at 20 °C[a]

	BHDC/benzene			AOT/*n*-heptane		
$\omega°$	N_a	r_w	σ	N_a	r_w	σ
8.5				115	18.6	
10	292	27.5	32.7			
11	70	22				
11.4				108	20.7	49.7
15				180	26.8	50.3
18				255	32	50.6
19.5				268	33.5	52.5
20	677	45.9	39.2	230	31.8	
21.2				314	36.3	52.6
23.6				350	39	54.5
26.3				409	42.4	55.8
30	1297	65.3	41.3			
30.3				520	48.3	56.4
35	1463	71.6	43.9			
40	1890	81.5	44.2	920	64	
49.4				1300	76.4	
66.7				1820	95.35	

[a] Aggregation number (N_a), radius of the water pool (r_w, Å), and surface area (σ, Å^2) per surfactant molecule at the surface of the water pool; BHDC (0.27 M) in benzene[20,21] and AOT (0.15 M) in *n*-heptane.[23,40] If necessary, the values of N_a and r_w were interpolated or extrapolated from the cited references.

carbon. Blank experiments were performed either in pure TMB/hydrocarbon solutions or in reverse micelles, in absence of TMB. No absorption was then detected either at 474 nm (TMB^+) or 720 nm (e^-_{aq}), in both deaerated solutions. Hence, the absorptions monitored at these two wavelengths in TMB/reverse micellar solutions arised only from monophotonic ionization of the TMB molecules located at the interface.

Absorption and emission spectra were recorded on a Perkin-Elmer λ_9 spectrophotometer and Fluorolog 111 spectrofluorimeter.

Results and Discussion

1. Estimation of the Electrical Potential at the Interface. The inner surface of a reverse micelle can display an electrical charge, owing to the dissociation of the ionic surfactant molecules in the vicinity of water. Hence, the net charge sets up an electrical potential which is nonuniform inside the water pool. Theoretical calculations[24,25] underlined the effect both of $\omega°$ and of the interfacial dielectric constant (ϵ_{eff}) on the variations of the electrical potential ($\Delta\psi$). A significant increase of the absolute value of the potential was found either with decreasing the constant ϵ_{eff} or with increasing the water pool size of AOT/isooctane micelles.

In order to obtain an estimation of ϵ_{eff} and $\Delta\psi$ variations, experiments are carried out using PyCHO, which appears to be a suitable probe: PyCHO is neutral, it is practically nonfluorescent in apolar organic solvents,[26] and its hydrophilic group favors its anchoring at the micellar surface. When dissolved in alcohol or dioxane−water mixtures, PyCHO exhibits a strong luminescence whose intensity (l_f) and maximum wavelength (λ_f) depend on the solvent dielectric constant;[26] the significant red shifts of λ_f display a linear relationship with an increase of the solvent polarity (curve 3 in ref 26), provided that the dielectric constant of the medium is greater than 10.

Hence, under the same experimental conditions, the intensity (l_f) and the position of λ_f are recorded in *reverse* (AOT and BHDC) and *direct* (NaLS and Brij 35) micelles for which the variations of the interfacial potential ($\Delta\psi$) are known[5] otherwise. Table 2 shows a little red shift of λ_f (2−3 nm) in reverse micelles on going from $\omega° = 18$ to $\omega° = 40$. This increase of the interfacial polarity with the micellar size is in agreement with previous results,[27] and it can be noticed that the surface area (σ) per surfactant headgroup becomes larger at the same time (cf. Table 1). For direct micelles, the decrease in surface polarity with increasing micellar aggregation number has been interpreted as a decrease in surface area per headgroup.[28] This opposite trend of σ variation between reverse micelles and direct micelles might probably result from the opposite sign of the curvature radius between these two kinds of micelles.

TABLE 2: Variation of the Maxima of Absorption (λ_{abs}, nm) and of Fluorescence (λ_f, nm) for Pyrenecarboxaldehyde (PyCHO) in Some Direct and Reverse Micelles and Estimation of the Interfacial Dielectric Constant (ϵ_{eff}) and of the Variations ($\Delta\psi$, mV) of the Interfacial Potential

micelles	$\omega°$	λ_{abs}	λ_f	ϵ_{eff}	$\Delta\psi$
NaLS			456	48	−150
NalS + LiCl 0.4 M			454	44	−115.5
NaLS + LiCl 0.6 M			453	42	−106
NaLS + NaCl 0.4 M			453	42	−104.2
NaLS + NaCl 0.6 M			452		−96.5
NaLS + CsCl 0.075 M			453		−110
NaLS + CsCl 0.125 M			453.5		−99
$Brij_{35}$			447	30	0
AOT/*n*-heptane	18	363	450	35.6	−52
AOT/*n*-heptane	40		452	40	−85
AOT/*n*-heptane + NaCl 0.2 M	18		446	28	7
BHDC/benzene	18	364	425		
BHDC/benzene	40		427		

A further analysis of Table 2 indicates that λ_f values, measured in BHDC micelles, display an important blue shift (∼25 nm), located outside the calibration curve of ref 26; in our opinion, the ϵ_{eff} determination, using PyCHO as a probe, seems unmeaning in BHDC micelles. Nevertheless, in a qualitative way and from the comparison between σ values for AOT and BHDC molecules (Table 1), an increase of the interfacial polarity on going from positively to negatively charged interfaces could be expected in reverse micelles, as observed in direct micelles.[26,28]

The λ_f, measured in anionic micelles, are translated into an ϵ_{eff} value (Table 2) on the basis of curve 3 from ref 26. From Table 2, it appears that direct NaLS micelles display a more polar interface ($\epsilon_{eff} \approx 48-42$) than reverse AOT micelles, where ϵ_{eff} is found about 35.6 and 40 for $\omega° = 18$ and 40, respectively. The difference in interfacial polarity between direct and reverse micelles is corroborated by an enhancement of the fluorescence intensity observed in direct micelles.

On the other hand, a model, proposed by Gaboriaud[29] for NaLS micelles, takes into account the specificity of the added counterions and allows the estimation of $\Delta\psi$ variations on addition of various electrolytes. Thus, with a value of −150 mV for a 0.1 M NaLS micellar solution, $\Delta\psi$ variations upon electrolyte additions were evaluated[5] and are reported in Table 2. The plot of λ_f, measured in various NaLS micelles, versus $\Delta\psi$ variations displays a linear relationship (Figure 1). The λ_f value measured for the nonionic direct micelle (Brij 35) also falls on the same straight line. With the assumption that the PyCHO molecule, in direct and reverse anionic micelles, is solubilized in a similar position at the interface, the λ_f location in AOT micelles leads to a potential of about −52 and −85 mV for $\omega° = 18$ and $\omega° = 40$, respectively, i.e. a $\Delta\psi$ variation of about −33 mV. This low $\Delta\psi$ value, observed in AOT reverse micelles, is explained by the high concentration of the Na^+ counterions in the water pool, 0.81 M ($\omega° = 18$) and 0.39 M ($\omega° = 40$), which screens the ionic charge of the headgroups. From Table 2, we can remark that the addition of 0.2 M NaCl to an AOT reverse micelle ($\omega° = 18$) leads to a nearly neutral micelle ($\Delta\psi \approx 7$ mV).

A similar $\Delta\psi$ value is obtained taking TMB as an acid−base indicator in AOT micelles (see next section). The variation of the electrostatic surface potential ($\Delta\psi$) can be evaluated from

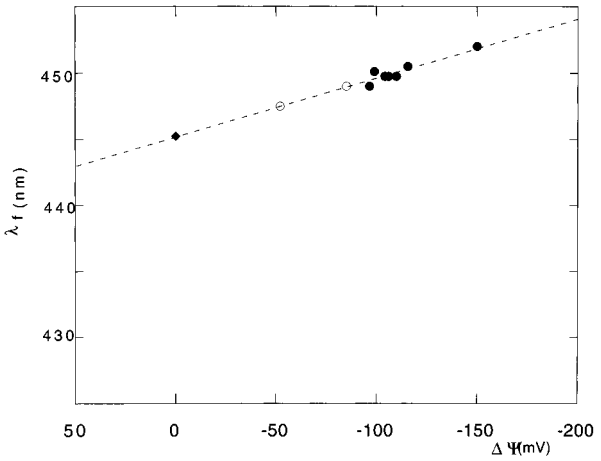

Figure 1. Variation of the maximum of fluorescence of PyCHO (λ_f in nm) versus the variations of the interfacial electrical potential ($\Delta\psi$ in mV) in direct micelles, NaLS (●) and Brij$_{35}$ (♦) and in reverse AOT micelles (○); $\omega^\circ = 18$ and 40.

the shift of pK_a (ΔpK) of a pH indicator solubilized at the micelle surface, using the following expression[30]

$$\Delta\psi = 0.06(\Delta pK) \quad (1)$$

$$\log I = pH_{eff} + pK_a \quad (2)$$

where $I = [TMBH^+]/[TMB_{int}]$ and, assuming that all H^+ are localized in the water pool, pH_{bulk} could be approximated to pH_{eff} according to ref 31.

As the respective concentration of the TMB molecules bound to the interface (TMB_{int}) and of the protonated form $TMBH^+$ were known versus the pH (pH_{bulk} range $4 \le pH \le 2.2$), the plot of log I versus pH_{eff} allows the pK_a determination by reading off the pH_{eff} at which log I = 0. The following pK_a values are thus obtained: −1.56 ($\omega^\circ = 20$) and −0.89 ($\omega^\circ = 40$). The corresponding ΔpK of ∼0.67 leds to $\Delta\psi$ variation ∼40 mV, a value in reasonable agreement with the above $\Delta\psi$ estimation of 33 mV, obtained from PyCHO measurements. It can be added that the increase of the water pool shifts the equilibrium toward the protonated form at a lower hydrogen concentration. The pK_a value of TMB in reverse micelles is considerably lower than those in direct anionic micelles,[19,32] showing that the dominant electrostatic interactions in AOT micelles appear to be those between the SO^{3-} and the added protons.

2. Determination of the Number of TMB Solubilized at the Interface. Neutral TMB is highly hydrophobic and dissolves essentially into the organic continuum medium. The position of its absorption maximum (λ_{abs}) is located at 304 and 315 nm in *n*-heptane and benzene solutions, respectively. The λ_{abs} is not significantly affected by dissolving TMB in reverse micelles, whatever the ω° value.

In order to correctly interpret the effect of ω° on the charge separation efficiency, it is necessary to determine the number of TMB molecules bound to the interface (TMB_{int}) which only are "photoionizable" in our experimental conditions. In the present work, two chemical reactions have been studied as a function of the pH of the water pool: (i) the protonation of TMB, leading to the $TMBH^+$ and $TMBH_2^{2+}$ formation in AOT micelles and (ii) the oxidation of the probe by ClO_4^- in BHDC micelles. The assumptions made are that the reverse micelles are spherical and monodisperse and that the extinction coefficient of the various species are not significantly modified on going from homogeneous to micellar solutions.

a. Anionic Micelles: Protonation of TMB. In aqueous solutions, TMB participates in protonation−deprotonation equilibria and it was observed that the micellar surface affects such

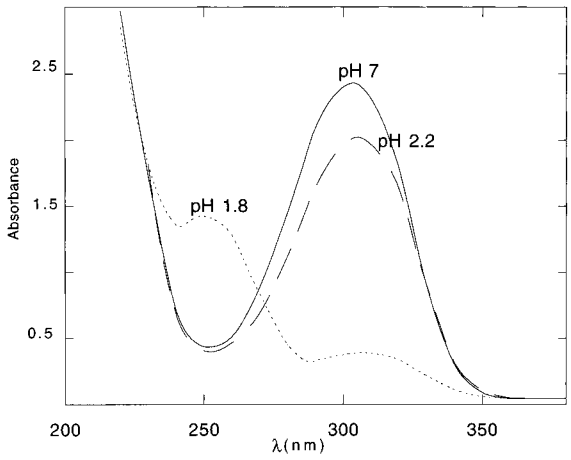

Figure 2. Absorption spectra of TMB in AOT/*n*-heptane micelle ($\omega^\circ = 20$) as a function of pH of the water pool: 7 (solid line), 2.2 (- - -), 1.8 (···).

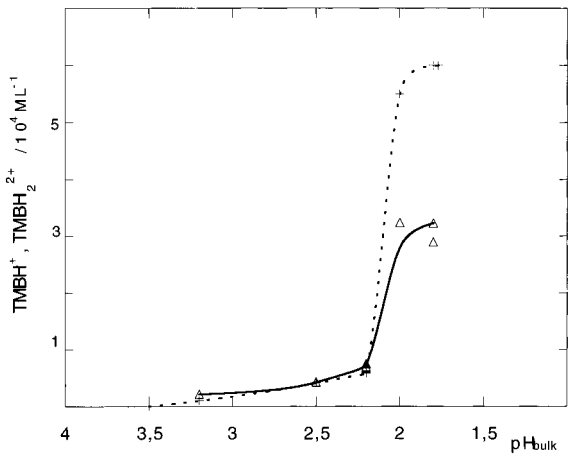

Figure 3. Variation of the concentration of $TMBH^+$ and $TMBH_2^{2+}$ (M L^{-1}) in AOT micelles as a function of pH of the water pool: $\omega^\circ = 20$ (△−△), $\omega^\circ = 40$ (+···+).

$$TMB \overset{H^+}{\leftrightarrow} TMBH^+ \overset{H^+}{\leftrightarrow} TMBH_2^{2+} \quad (3)$$

equilibria in direct micelles.[19,32]

In AOT/*n*-heptane micelles, TMB exhibits an absorption peak at 304 nm, $TMBH^+$ at 316 nm, and $TMBH_2^{2+}$ at 250 nm. The analysis of the electronic absorption spectra, obtained at various ω° ($10 \le \omega^\circ \le 40$) versus the pH_{bulk} of the added HCl solution shows the presence of isosbestic points which reveal that the transformation induced by the change of pH is a simple process from one form to another. In the pH_{bulk} range ($4 \le pH \le 2.2$), only $TMBH^+$ is formed, while the two protonated species—$TMBH^+$ and $TMBH_2^{2+}$—are present for $2 \le pH \le 1.8$ (Figure 2); it is also found that the smaller the ω°, the lower the pH of $TMBH_2^{2+}$ formation. Below pH 1.6 (depending on the ω° value), the absorption spectrum displays a large scattering contribution, resulting probably from a modification of the micellar size upon acid addition.

In the pH_{bulk} range $3.5 \le pH \le 1.5$, by following either the depletion of the TMB absorption at 304 nm or the change of the absorbance at 250 nm ($TMBH_2^{2+}$) and 316 nm ($TMBH^+$), the variations of the absorption versus pH are represented by sigmoid curves, reaching a similar limit value whatever the mode of determination (Figure 3); this finding suggests that the added $[H_3O^+]$ should be so efficient that practically all TMB_{int} have reacted. We have also checked whether the oxidation of TMB by Cl^-, leading to TMB^+, occurs: a very low concentration of

TABLE 3: Average Number of TMB_{int} Molecules per Micelle at Various $\omega°$ Values for AOT/*n*-Heptane and BHDC/Benzene

$\omega°$	AOT/*n*-heptane	BHDC/benzene
10	0.3	0.05−0.06
20	0.58−0.65	0.18
25		0.30
30	2.17	0.35
35		0.39
40	3.37−3.68	0.73

the oxidized form TMB^+ is detected (about 10^{-7} M), which is negligible as compared with the concentrations of the two protonated forms. The percentage of interfacial TMB (TMB_{int}) with respect to the overall TMB (TMB_{tot}) incorporated in the solution is found to be about 30−40% of TMB_{tot}, within the experimental accuracy (15−20%) of these sets of measurements.

The data summarized in Table 3 (column 2) give the average number of TMB_{int} per AOT micelle. The relative concentration of TMB_{int} and micelles are such that in one pool the number of solubilized TMB was of about 0.3 molecule at $\omega° = 10$, and 3.5 at $\omega° = 40$, respectively. These values are consistent with the earlier observation by Mori[33] who estimated the average number of another hydrophobic probe—the pyrene sulfonate (PSA)—solubilized in one water pool of AOT micelles to be about 0.3 ($\omega° = 20$) and 1.4 ($\omega° = 50$). On $\omega°$ variation (Figure 4), it can be observed that the number of TMB_{int} per micelle parallels the variation of the square radius of the water pool $(r_w)^2$. Such a dependence corroborates the adsorption of TMB_{int} on the surface of monodispersed colloidal particles.

b. Cationic Micelles: Oxidation of TMB. Unfortunately, it was not possible to produce chemically the anionic amine oxide ($TMBN^+O^-$) in cationic micelles. Addition of H_2O_2 led also to the destruction of the micelle.

The TMB oxidation by the anion ClO_4^- ($HClO_4$ solution) is undertaken as a function of pH and $\omega°$. The analysis of the absorption spectra, obtained in presence of $HClO_4$, has shown that the monoprotonation and diprotonation of TMB do not occur, as expected; a new single absorption band, located at 466 nm, characteristic of TMB^{2+},[34,35] appears, and a decrease of the absorbance of neutral TMB (315 nm) is observed at the same time.

As for the AOT micelles, the TMB_{int} concentration is evaluated either by the depletion of the TMB absorption band or by the appearance of the TMB^{2+} absorption ($\epsilon_{474} = 7.10^4$ M^{-1} cm^{-1}).[35] In spite of the presence of an isosbestic point at 400 nm, there is considerable scatter in the results, obtained from these two different modes of evaluation: on TMB^{2+} measurements, the concentration of TMB_{int} is found about one order of magnitude lower than that on TMB consumption; the destabilization of the TMB^{2+} species by the positive interface as well as its rapid decomposition[35,36] give a plausible explanation to this discrepancy. So, the determination of the number of TMB_{int} molecules, bound to the BHDC interface, is based on the decrease of the absorbance at 315 nm, carefully corrected from the low contribution of TMB^{2+} to the absorption spectrum ($\epsilon_{TMB^{2+}} \approx 25\,000$ M^{-1} cm^{-1} at 315 nm). Figure 5 demonstrates that the number of TMB_{int} in BHDC micelles is proportional to the surface of the water pool as in AOT micelles; it also shows that the average number of TMB_{int} at the positive interface is kept small compared to that of the anionic ones (Table 3): only 10% of the TMB_{tot} are bound to the cationic interface, although the r_w value is greater in BHDC than in AOT micelles. This finding can be explained by the influence of the solvent on the partitioning of the TMB molecule among the surfactant layer and the oil; it is effectively found that the TMB solubility in benzene is 3-fold greater than in *n*-heptane.

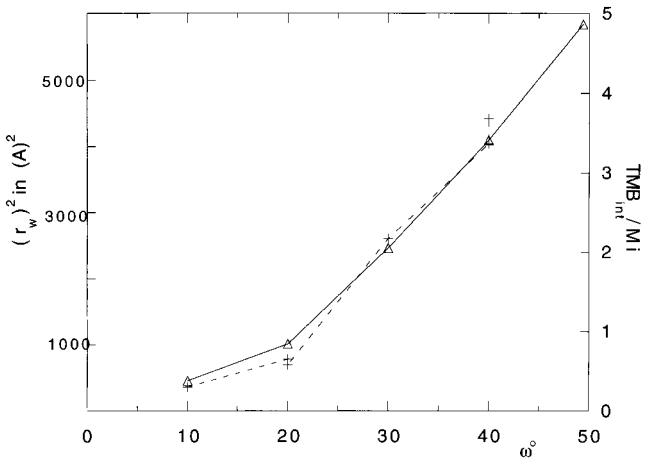

Figure 4. Variations of the number of TMB_{int} molecules per AOT micelle (+···+) and of the square radius of the water pool, r_w^2 in Å^2, (△−△) versus $\omega°$.

Furthermore, the variation in the composition of the hydrophobic binding sites might also affect their interaction with the probe; the bulky character of the phenyldimethyl ammonium of BHDC molecule, as opposed to the anionic sulfate groups of an AOT molecule, might partly hinder the penetration of the dimethylamino group of the TMB into the interface. Effectively, NMR measurements displayed a location of the phenyl group between the surfactants headgroups, away from the water phase.[21]

From these sets of experiments, it can be concluded that the surface structure of the interface and the solvent play an important role in determining the number of probably the orientation of the probe molecule as well as the water penetration. The local structure of the interface and its dielectric property are thus expected to influence the behavior of the solute located at the interface.

3. Charge Separation Efficiency: Effect of $\omega°$. As the photoionization occurs on the time scale of an electronic transition (10^{-15}−10^{-16} s), the probe location at the micellar interface can be considered as frozen with respect to the intermicellar reactions (10^{-10}−10^{-8} s).[20,37] Under monophotonic excitation, the TMB_{int} solubilized at the interface undergoes triplet formation and photoionization according to[7]

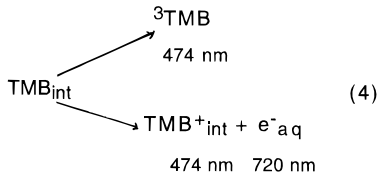

In reverse micelles, the TMB^+ radical cation displays a relative stability whose lifetime τ depends on the $\omega°$ value; we observe that τ_{TMB^+} is not significantly altered by the presence of oxygen. In deaerated solutions, TMB^+ disappears in less than a second, whereas the lifetime of the e^-_{aq} is considerably shorter (in the microsecond scale), as expected by the presence of the micellar interface which prevents the back reaction and in agreement with literature data.[9,11,12]

In order to discriminate the photocation absorption from that of the ^{3}TMB, the optical density at 474 nm is monitored at 2 μs, before the TMB^+ decay, in presence of oxygen which is known for quenching the triplet state.[7]

Figure 6 displays the yield of the produced photocation (Y_{TMB^+}), i.e. the number of TMB^+ with respect to the number of TMB_{int} as a function of $\omega°$ in AOT (curve a) and in BHDC (curve b) micellar solutions. From the present data, (i) it seems obvious that, in anionic reverse micelles, the highest efficiencies for charge separation are not associated with the most negative

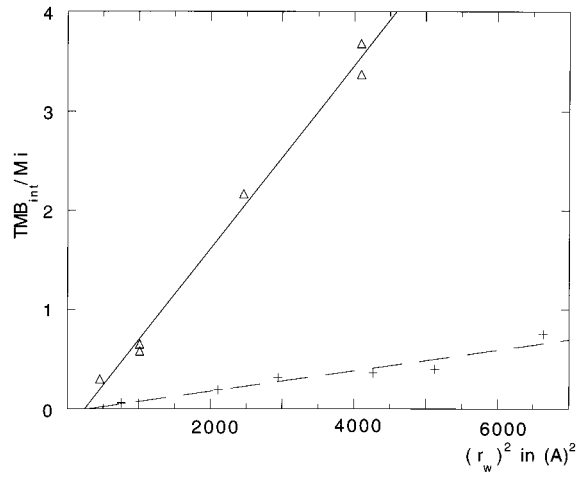

Figure 5. Variations of the number of TMB_{int} molecules per AOT micelle (△−△) and BHDC micelle (+-+) versus the square radius of the water pool in Å^2.

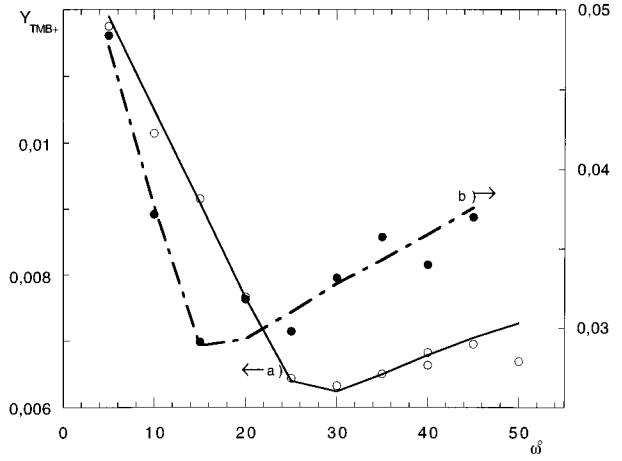

Figure 6. Variation of the photoionization yield (Y_{TMB^+}), expressed as the concentration ratio of TMB^+ with respect to TMB_{int}, versus $\omega°$. In AOT, curve a (○−○), and in BHDC, curve b (●- -●), micelles.

interface potentials, contrary to the situation which prevails in direct negative micelles.[5] In AOT micelles, a negative $\Delta\psi$ drop of about 40 mV—as estimated above, between $\omega° = 18$ and $\omega° = 40$—slightly affects the Y_{TMB^+} value in AOT micelles, whereas for the same $\Delta\psi$ drop Y_{TMB^+} increases by an order of magnitude in direct NaLS micelles.[6] Furthermore, as the degree of counterion binding decreases with increasing $\omega°$, a less negative potential should be expected at $\omega° = 5$ than at $\omega° = 40$; the present experiments clearly show that an opposite trend of Y_{TMB^+} variation is observed in this $\omega°$ range.

On the basis of e^-_{aq} determinations, it was shown[38] that the efficiency of electron capture by the pools increases with the availability of free water in the pool; in other words, as observed in direct swollen micelles,[6] the nature of the core would be the main parameter which might control the intramicellar recombination.

(ii) Surprisingly at first sight, in spite of the positive charge of the interface which would "destabilize" the TMB^+ species, Y_{TMB^+} is found 6-fold greater in BHDC than in AOT micelles, whereas the overall photoionization yield is roughly 15 times smaller in direct cationic than in direct anionic micelles.[6] A schematic representation of the $\Delta\psi$ variations on the distance "*x*" from the membrane to the center of the water pool—where the electron solvation probably occurs—is depicted in Figure 7. According to the symmetry condition of the reverse micelle and to the sign of the interfacial charge, the potential profile is then found to go through a maximum in negative micelles or

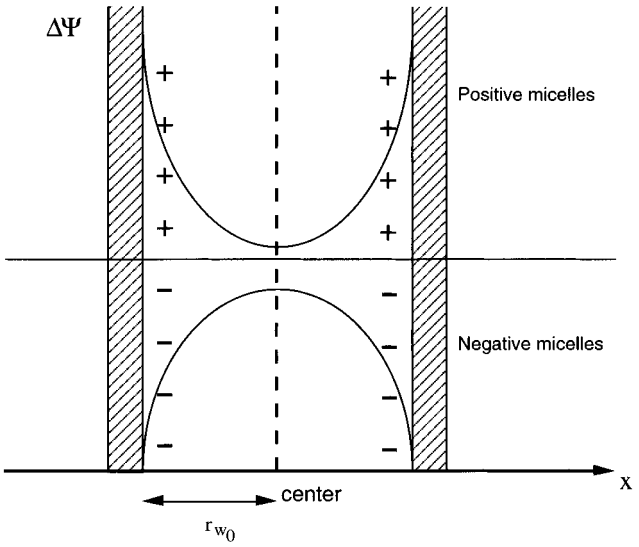

Figure 7. Schematic representation of the potential profile on the distance "*x*" from the membrane to the center of the water pool.

to a minimum in positive ones. In other words, before its solvation, the photoelectron produced at the membrane surface will sense a potential well in BHDC micelles, whereas in AOT micelles, the photoelectron has to overcome a potential barrier. As the potential becomes more negative on $\omega°$ increase (see part 1), such a potential barrier slightly increases with the micellar size and it would delay the electron solvation into the aqueous core. In anionic AOT micelles, Gauduel[12] has effectively observed that the apparent rise time of the absorption of the fully solvated electron (e^-_{aq}) increases with $\omega°$. The ultrafast intramicellar geminate recombinations, between the photocation and the photoelectron, could be indirectly inferred from this observation. At the interface, the ions are mostly solvated by the water. With respect to the sign of the interface charge, it is intuitively expected that the TMB^+ species is buried deeper in BHDC than in AOT micelles, and TMB^+ being pulled toward the oil phase, further away from the photoelectron which is pushed toward the water core. Hence, the presence of a potential well, associated to the mean distance between the photoelectron and the TMB^+ species, might prevent the recombinations in cationic reverse micelles; conversely, negative interfaces would promote the intramicellar geminate recombinations, leading thus to a lower Y_{TMB^+} value in AOT than in BHDC micelles. This opposite trend of Y_{TMB^+} variation on the sign of the interfacial charge between direct and reverse micelles might also reflect an effect of the curvature radius on the charge separation process.

(iii) The plot of Y_{TMB^+} versus $\omega°$ displays a minimum at about $\omega° = 25$ in AOT micelles, which is reminiscent of the variation of the free water fraction on $\omega°$ and reported for this micellar solution.[14] In the accuracy limit of the experimental determination of the number of TMB_{int} molecules, such a close agreement, as displayed in Figure 8, would be regarded as an inhomogeneous effect of the environment, which might be considered at the microscopic level.

On one hand, the liquid interfacial region is characterized by several nonuniform properties, such as density, viscosity, and ϵ_{eff}.

On the other hand, the ionization potential of a molecule in a given solvent (E_{th}) depends largely on the V_0 value in this solvent.[1−4] It was found that V_0 increases significantly on going from the liquid to the solid state or when the solvent static dielectric constant decreases.[2,3]

A pragmatic approach is to consider each interfacial region as a separate phase with a fixed V_0, different from the V_0 values

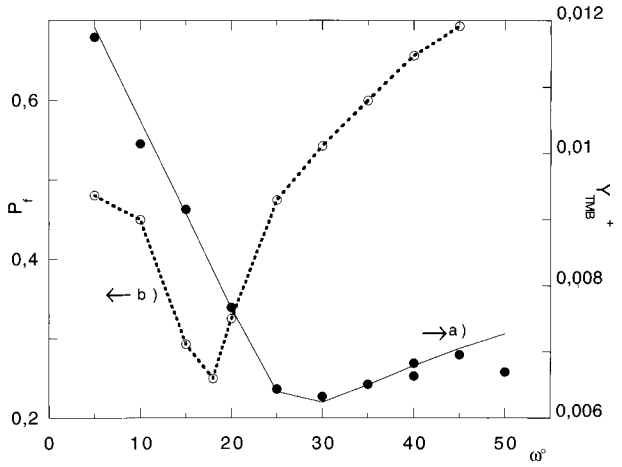

Figure 8. Variation of Y_{TMB^+} (curve a, ●−●) and of the fraction of free water P_f from ref 14 (curve b: (○···○) versus $\omega°$ in AOT micelles.

of the aqueous or hydrocarbon phase. Quantifying the part played by the packing of the headgroups and by the structure of water appears to be unaccessible in determining the physical properties of an interface and more precisely in the evaluation of the V_0 value of the excess electron. Nevertheless, as the trapped water fraction is negligible, in a rough approximation, we assume that V_0 (at a given $\omega°$) would be dependent on the relative fraction of bound and free water which displays an opposite variation on $\omega°$.[14] In AOT micelles, a trend of the V_0 variation on $\omega°$ is thus attempted, on the basis of $V_0 = -1.2$ eV in bulk water.[39] In the range $5 \leq \omega° \leq 20$, V_0 is found to increase on going from -0.6 eV ($\omega° = 5$) to -0.3 eV ($\omega° = 20$). As a result of the V_0 increase ($\sim$0.3 eV) with $\omega°$, the photoionization energy threshold (E_{th}) of TMB should be shifted to the blue; as the cross-section of photoionization depends on the excess energy available above E_{th}, a corresponding decrease of Y_{TMB^+} might be expected at $\omega° = 20$. Conversely, in the range $20 \leq \omega° \leq 40$, the increase of the fraction of free water would induce a decrease in the V_0 value, hence E_{th} would be shifted to the red, involving both an increase of the kinetics energy of the photoelectron and hence of the Y_{TMB^+} value.

In BHDC micelles, if the presence of bound and free water was also evidenced in the aqueous core,[21] the relative fraction of each kind of water has not been determined to our knowledge and does not permit the same approach in an approximation of V_0. By analogy with AOT micelles, Y_{TMB^+} variations versus $\omega°$ in BHDC solutions are also ascribed to changes in the V_0 values. The present data also underline that $\omega° \approx 20$ is decisive in the change of water properties as well as in charge separation and electron solvation processes, whatever the nature of the surfactant. As a final remark, the shape of the Y_{TMB^+} curve as a function $\omega°$ seems slightly flattened in anionic micelles. This difference in shape might be resulted either from different relaxation channels of the excited singlet state (further experiments will be undertaken) or from an effect of the interface compactness.[41]

Conclusion

The agreement between luminescence and the ΔpK experiments clearly show that the water pool size slightly modifies the electric field gradient at the micelle surface. The $\Delta\psi$ variations are limited by the high concentration of the counterions in the water pool.

By taking advantage of the fact that the probe molecules located at the interface only give rise to photoionization, this present work also demonstrates that the $\Delta\psi$ variations in reverse micelles do not control the charge separation efficiency. The importance of the molecular structure of the water pool, in modifying the fundamental energy of the excess electron (V_0) and hence the photoionization threshold (E_{th}), might be a determinant parameter in the charge separation process.

Besides the influence of the water core, the present work has also underlined the important role of the host structure which controls more or less the penetration of water and the concentration of reagents at the reaction site.

Acknowledgment. We thank Dr. S. Hautecloque for valuable discussions.

References and Notes

(1) (a) Raz, B.; Jortner, J. *Chem. Phys. Lett.* **1969**, *4*, 155. (b) Holroyd, R. A.; Tames, S.; Kennedy, A. *J. Phys. Chem.* **1975**, *79*, 2857.
(2) Bullot, J.; Gauthier, M. *Can. J. Chem.* **1977**, *55*, 1821.
(3) Grand, D.; Bernas, A. *J. Phys. Chem.* **1977**, *81*, 1209.
(4) Bernas, A.; Grand, D.; Hautecloque, S.; Chambaudet, A. *J. Phys. Chem.* **1981**, *85*, 3684.
(5) Hautecloque, S.; Grand, D.; Bernas, A. *J. Phys. Chem.* **1985**, *89*, 2705.
(6) Bernas, A.; Grand, D.; Hautecloque, S. *Radiat. Phys. Chem.* **1988**, *32*, 309.
(7) Alkaitis, S. A.; Gratzel, M. *J. Am. Chem. Soc.* **1976**, *98*, 3549.
(8) Grand, D. *J. Phys. Chem.* **1990**, *94*, 7585.
(9) Calvo-Perez, V.; Beddard, G. S.; Fendler, J. H. *J. Phys. Chem.* **1981**, *85*, 2316.
(10) Gauduel, Y.; Migus, A.; Martin, J. L.; Antonetti, A. *IEEE J. Quantum Electron.* **1984**, *20*, 1370.
(11) Abdel-Kader, M. H.; Krebs, P. *J. Chem. Soc., Faraday Trans. 1*, **1988**, *84*, 2241.
(12) Gauduel, Y.; Pommeret, S.; Yamada, N.; Migus, A.; Antonetti, A. *J. Am. Chem. Soc.* **1989**, *111*, 4974.
(13) Wong, M.; Gratzel, M.; Thomas, J. K. *Chem. Phys. Lett.* **1975**, *30*, 329.
(14) Jain, T. K.; Varshney, M.; Maitra, A. *J. Phys. Chem.* **1989**, *93*, 7409.
(15) D'Aprano, A.; Lizzio, A.; Liver, V. T.; Aliotta, F.; Vasi, C.; Migliardo, P. *J. Phys. Chem.* **1988**, *92*, 4436.
(16) Hauser, H.; Haering, G.; Pande, A.; Luisi, P. L. *J. Phys. Chem.* **1989**, *93*, 7869.
(17) Wong, M.; Thomas, J. K.; Gratzel, M. *J. Am. Chem. Soc.* **1976**, *98*, 2391.
(18) Fulton, A.; Lyons, L. E. *Aust. J. Chem.* **1968**, *21*, 873.
(19) Hashimoto, S.; Thomas, J. K. *J. Phys. Chem.* **1984**, *88*, 4044.
(20) Jada, A. Thesis, Strasbourg, France, 1984.
(21) McNeil, R.; Thomas, J. K. *J. Colloid Interface Sci.* **1981**, *83*, 57.
(22) Maitra, A. *J. Phys. Chem.* **1984**, *88*, 5122.
(23) Cabos, C.; Marignan, J. *J. Phys. Lett.* **1987**, *46*, L-267.
(24) Karpe, P.; Ruckenstein, E. *J. Colloid Interface Sci.* **1990**, *137*, 408.
(25) Tomic, M.; Kallay, N. *J. Phys. Chem.* **1992**, *96*, 3874.
(26) Kalyanasundaram, K.; Thomas, J. K. *J. Phys. Chem.* **1977**, *81*, 2176.
(27) Wong, M.; Thomas, J. K.; Nowak, T. *J. Am. Chem. Soc.* **1977**, *99*, 4730.
(28) Zachariasse, K. A.; Van Phuc, N.; Kozankiewicz, B. *J. Phys. Chem.* **1981**, *85*, 2676.
(29) Charbit, G.; Dorion, F.; Gaboriaud, R. *J. Chim. Phys.* **1984**, *81*, 187.
(30) Fernandez, M. S.; Fromherz, P. *J. Phys. Chem.* **1977**, *81*, 1755.
(31) ElSeoud, O. A.; Chinelatto, A. M.; Shimuzu, M. R. *J. Colloid Interface Sci.* **1982**, *88*, 420.
(32) Beck, S. M.; Brus, L. E. *J. Am. Chem. Soc.* **1983**, *105*, 1106.
(33) Mori, Y.; Yoneda, A.; Shinoda, H.; Kitagawa, T. *Chem. Phys. Lett.* **1991**, *183*, 584.
(34) Hasegawa, H. *J. Phys. Chem.* **1961**, *65*, 292.
(35) Saget, J. P.; Plichon, V. *Bull. Soc. Chim. Fr.* **1969**; 1393.
(36) Kobayashi. *Denki Kagaku oyobi Kogyo* **Butsuri Kagaku 1990**, *58*, 465.
(37) Jada, A.; Lang, J.; Zana, R. *J. Chim. Phys.* **1989**, *93*, 10.
(38) Bakale, G.; Beck, G.; Thomas, J. K. *J. Phys. Chem.* **1981**, *85*, 1062.
(39) Bernas, A.; Grand, D.; Amouyal, E. *J. Phys. Chem.* **1980**, *84*, 1259.
(40) Lang, J.; Jada, A.; Malliaris, A. *J. Phys. Chem.* **1988**, *92*, 1946.
(41) Kikuchi, K.; Thomas, J. K. *Chem. Phys. Lett.* **1988**, *148*, 245.